JCTC Journal of Chemical Theory and Computation
Article
Cite This: J. Chem. Theory Comput. 2019, 15, 303−310
pubs.acs.org/JCTC

Generalized Gradient Approximation Exchange Energy Functional with Near-Best Semilocal Performance

Javier Carmona-Espíndola,*,† José L. Gázquez,*,‡ Alberto Vela,§ and S. B. Trickey‖

†Departamento de Química, CONACYT-Universidad Autónoma Metropolitana-Iztapalapa, Av. San Rafael Atlixco 186, Ciudad de México 09340, México

‡Departamento de Química, Universidad Autónoma Metropolitana-Iztapalapa, Av. San Rafael Atlixco 186, Ciudad de México 09340, México

§Departamento de Química, Centro de Investigación y de Estudios Avanzados, Av. Instituto Politécnico Nacional 2508, Ciudad de México 07360, México

‖Quantum Theory Project, Department of Physics and Deptartment of Chemistry, University of Florida, P.O. Box 118435, Gainesville, Florida 32611-8435, United States

Supporting Information

ABSTRACT: We develop and validate a nonempirical generalized gradient approximation (GGA) exchange (X) density functional that performs as well as the SCAN (strongly constrained and appropriately normed) meta-GGA on standard thermochemistry tests. Additionally, the new functional (NCAP, nearly correct asymptotic potential) yields Kohn−Sham eigenvalues that are useful approximations of the density functional theory (DFT) ionization potential theorem values by inclusion of a systematic derivative discontinuity shift of the X potential. NCAP also enables time-dependent DFT (TD-DFT) calculations of good-quality polarizabilities, hyper-polarizabilities, and one-Fermion excited states without modification (calculated or ad hoc) of the long-range behavior of the exchange potential or other patches. NCAP is constructed by reconsidering the imposition of the asymptotic correctness of the X potential ($-1/r$) as a constraint. Inclusion of derivative discontinuity and approximate integer self-interaction correction treatments along with first-principles determination of the effective second-order gradient expansion coefficient yields a major advance over our earlier correct asymptotic potential functional [CAP; *J. Chem. Phys.* **2015**, *142*, 054105]. The new functional reduces a spurious bump in the CAP atomic exchange potential and moves it to distances irrelevantly far from the nucleus (outside the tail of essentially all practical basis functions). It therefore has nearly correct atomic exchange-potential behavior out to rather large finite distances r from the nucleus but eventually goes as $-c/r$ with an estimated value for the constant c of around 0.3, so as to achieve other important properties of exact DFT exchange within the restrictions of the GGA form. We illustrate the results with the Ne atom optimized effective potentials and with standard molecular benchmark test data sets for thermochemical, structural, and response properties.

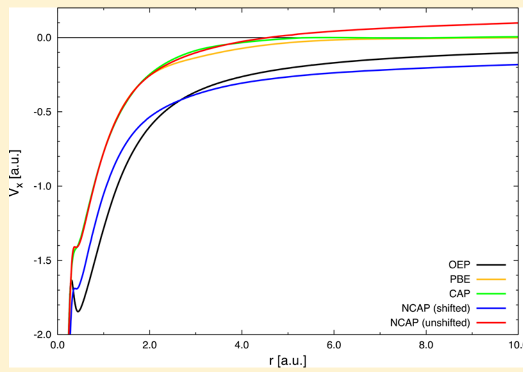

I. INTRODUCTION

Pursuit of balance between accuracy and computational cost has driven the development of constraint-based exchange−correlation (XC) functionals to an emphasis on meta-generalized gradient approximation (meta-GGA) functionals, i.e., functionals that depend upon the electron density $n(\mathbf{r})$, its gradient, and the positive-definite Kohn−Sham (KS) kinetic energy density. Apparently, the most successful meta-GGA so far is SCAN (strongly constrained and appropriately normed).[1] A comparatively unexplored issue is to what extent a simple GGA functional can meet or exceed the performance of such a high-quality meta-GGA on standard tests. We and colleagues[2−5] have explored the GGA rung of the Perdew−Schmidt ladder XC functionals[6] because such functionals have great computational utility, they are intrinsically relevant to orbital-free density functional theory,[7] and they typically are an essential ingredient in higher rung XC functionals. By now it is incontrovertible that a constraint-based, nonempirical GGA can be constructed which is substantially superior[8−12] to the most popular one[13] on many standard molecular tests and always is competitive on such tests.

Heretofore no one has found rational design principles which yield a GGA that performs systematically almost as well as a modern meta-GGA on those common benchmarks. In this work, we achieve that goal. In the bargain, we provide a functional that also supports time-dependent DFT (TD-DFT) calculations of response properties (e.g., polarizabilities and

Received: October 3, 2018
Published: November 27, 2018

DOI: 10.1021/acs.jctc.8b00998
J. Chem. Theory Comput. 2019, 15, 303−310

hyper-polarizabilities) and one-electron excited states without alteration or long-range patching. The new functional also provides highest occupied molecular orbital (HOMO) energies that are reasonable approximations of the DFT ionization potential theorem.[14−17] To our knowledge no existing constraint-based meta-GGA achieves all three of those objectives. (Semiempirical XC functionals are not included in this discussion.)

Prior exploration[2−5] of GGA performance limitations has brought inherent ambiguities into focus. No GGA X functional can satisfy all the known X functional constraints, so progress depends on insightful choice. Furthermore, most constraints are for arbitrarily small or asymptotically large values of the reduced density gradient s in the usual GGA X expression[18]

$$E_X^{GGA}[n] = \int n(\mathbf{r})\, \varepsilon_X^{LDA}(n(\mathbf{r}))\, F_X(s)\, d\mathbf{r} \tag{1}$$

Here $\varepsilon_X^{LDA}(n(\mathbf{r})) = A_X(n(\mathbf{r}))^{1/3}$ is the LDA[19] for the exchange energy per particle, $A_X = -3(3\pi^2)^{1/3}/4\pi$, and $s(\mathbf{r}) = |\nabla n(\mathbf{r})|/2k_F(\mathbf{r})\, n(\mathbf{r})$, is the exchange reduced density gradient with $k_F = (3\pi^2 n(\mathbf{r}))^{1/3}$. For both small- and large-s regimes, there are incompatible constraints. Most relevant to the present discussion, there are contradictory constraints for $s \to \infty$.[2,4,5,13,18,20−26] Interpolation of $F_X(s)$ between the small- and large-s limits thus is inherently ambiguous; hence, many different GGAs have been contrived.

In ref 2 we presented the CAP (correct asymptotic potential) GGA. It was designed to achieve a balanced description of thermodynamic, kinetic, and structural molecular properties, and also of excitation energies, polarizabilities, and hyper-polarizabilities as measured by errors relative to standard data sets. For brevity we call the latter group "response properties and excitation energies". Popular GGA X functionals, e.g., PBE,[13] were designed primarily for the former properties, hence, on details of $F_X(s)$ on $0 \le s \le 3$. Such functionals have atomic X potentials that vanish improperly rapidly with radial distance. But response properties and excitation energies calculated via TD-DFT[27,28] require proper $-1/r$ decay. That forces $F_X(s)$ to diverge as $s \to \infty$. Therefore, the CAP enhancement factor was constructed to have a strong resemblance to the PBE enhancement factor on $0 \le s \le 3$ coupled with $F_X(s) \to (4\pi/3)s$ as $s \to \infty$.

The CAP X functional combined with the PBE C functional ("CAP-PBE") gives quite good performance on a wide variety of standard molecular tests.[2] Even better, when used with Born−Oppenheimer MD to treat temperature effects, it also does well on molecular response properties.[3] But it has two peculiarities that actually open a route to major improvement. First, the CAP X potential goes positive for moderately large distances (of the order 5−6 au) from an atomic nucleus; then it goes back to negative and evolves to the asymptotic $-1/r$ far from the origin (see figures in ref 2). In a finite $\mathcal{L}^2$ basis set, that positive bump stabilizes the lowest unoccupied molecular orbital (LUMO) even though it actually is a scattering state. Relative to an ordinary GGA value (e.g., from PBE), the LUMO energy thus goes up and the HOMO−LUMO gap is enlarged. That helps to improve the description of response properties and excitation energies. A similarly unphysical bump occurs in a GGA functional reported[26] shortly after ref 2. That functional scales the PBE GGA enhancement factor by an s-dependent factor that conforms to the $-1/r$ constraint. The scale factor was parametrized to experimental data on formaldehyde. In addition to having a bump, the resulting GGA X potential v_X also goes positive at large r. Earlier, Armiento and Kümmel[25] had introduced a GGA X functional, AK13, also designed to recover $-1/r$ behavior, hence also with a divergent enhancement factor, namely

$$F_X^{AK13}(s) = 1 + B_1^{AK13} s \ln(1+s) + B_2^{AK13} s \ln[1 + \ln(1+s)] \tag{2}$$

The KS orbitals and X potential from AK13 (used with PBE C) have several desirable properties but the AK13 energetics errors (e.g., in heats of formation) are not competitive with ordinary GGAs,[29−32] much less with highly evolved ones such as lsRBE-PW91.[4] AK13 also generates a small upward bump in, for example, the H atom v_X about where the v_X^{CAP} bump is but it comes from the $B_2^{AK13} s \ln[1 + \ln(1 + s)]$ term, a form not in F_X^{CAP}. Somewhat related behavior was found in the construction[33] of an approximate X hole via analysis of the weighted density approximation. When evaluated in the X-only case, the asymptotic behavior of the exchange potential they obtained goes as ($-$constant/r) with the constant in the range (0.5, 1].

The ambiguity of near-optimal GGA choice also has obscured an opportunity. For example, lsRPBE-PW91[4] is a PW91-like GGA X functional that, together with PW91 C,[34] delivers thermochemistry benchmark performance generally competitive with CAP-PBE. But for heats of formation, lsRPBE-PW91 is superior: mean absolute deviation (MAD) of 7.51 kcal/mol versus 9.23 kcal/mol for CAP-PBE. Thus, lsRPBE-PW91 is competitive with meta-GGAs and some semiempirical hybrid functionals: PBE and B3LYP values are 21.2 and 5.7 kcal/mol, respectively. But the lsRPBE-PW91 parametrization did not use the large-s constraint that corresponds to the $-1/r$ decay of $v_X(r)$, so lsRPBE-PW91 response property errors are like those of other GGAs parametrized with the same design choice and thus are inferior to CAP-PBE errors; see ref 3. The second unresolved issue therefore is if a GGA functional can combine the successes of lsRPBE-PW91 and CAP-PBE or whether, instead, one must have one type of GGA for response properties and excitation energies, and another for thermodynamic, kinetic, and structural molecular properties.

The functional presented here resolves both issues. In what follows, we outline the analysis of GGA sources of asymptotic $-1/r$ behavior, the prioritization and use of applicable constraints (including approximate correction for derivative discontinuity and imposition of the DFT ionization potential theorem[14−17]), details of computational methods for testing, and outcomes of testing.

II. EXCHANGE ENERGY FUNCTIONAL CONSTRUCTION

As discussed in the Supporting Information, $-1/r$ behavior in an atomic GGA X potential arises both structurally from the spherical coordinate Jacobian and from the asymptotic form of the atomic density,[16,35,36] which very far from the nucleus is dominated by the exponential decay,

$$n(r) \xrightarrow[r\to\infty]{} n_0 e^{-\lambda r} \qquad \lambda = 2\sqrt{-2\varepsilon_{HOMO}} \tag{3}$$

where n_0 is a system-dependent normalization constant and ε_{HOMO} is the HOMO eigenvalue. Substitution of this density form in the GGA $v_X^{GGA}([n];\mathbf{r})$ expression, retention of leading derivative terms, and imposition of equality with $-1/r$ give a second-order differential equation for F_X at large s. A structural contribution arises from the simplest candidate solution, $F_X(s) \xrightarrow[s\to\infty]{} C_0 s$ with C_0 a constant,[21]

$$v_X^{GGA}([n];\mathbf{r}) \xrightarrow[r\to\infty]{} -\frac{3C_0}{4\pi}\frac{1}{r} \tag{4}$$

independent of the asymptotic density decay. A second candidate is $F_X(s) \xrightarrow[s\to\infty]{} C_1 s \ln s$. With $C_1 = C_0$ and λ from (3), one has

$$v_X^{GGA}([n];\mathbf{r}) \xrightarrow[r\to\infty]{} \left(\frac{\sqrt{-2\varepsilon_{HOMO}}}{3} - \frac{1 + C_A}{r}\right) \tag{5}$$

where $C_A = \ln(\sqrt{-2\varepsilon_H}/(3\pi^2 n_0)^{1/3})$.

The potential shift in (5) has been discussed for the AK13 functional.[25,29−32] It is related in both cases to the derivative discontinuity of the KS potential.[14,15,17,37,38] Note that the actual $-(1 + C_A)/r$ has two contributions, $-1/r$ that has a structural origin and $-C_A/r$ that comes from the asymptotic behavior of the density.

The most obvious enhancement factor obtainable from eqs 4 and 5 is a simple linear combination

$$F_X^{trial}(s) = \frac{4\pi}{3}[(1-\zeta)s\ln(1+s) + \zeta s] \tag{6}$$

$$v_X^{trial}([n];\mathbf{r}) \xrightarrow[r\to\infty]{} v_X^{trial}(\varepsilon_{HOMO},\zeta) - \frac{(1-\zeta)C_A}{r} - \frac{1-\zeta}{r} - \frac{\zeta}{r} \tag{7}$$

with ζ a constant. This form is set entirely by asymptotics without regard to small-s behavior, in particular the coefficient in $F_X^{trial}(s) = 1 + \mu s^2 + ...$ It is unsurprising therefore that (6) does badly on standard thermochemistry tests.

A GGA enhancement factor form that incorporates the foregoing limiting behavior approximately yet behaves like a successful GGA (e.g., lsRPBE) at small and intermediate s and has the proper small-s limit is

$$F_X^{NCAP}(s) = 1 + \mu \tanh(s)\sinh^{-1}(s) \times \frac{1 + \alpha((1-\zeta)s\ln(1+s) + \zeta s)}{1 + \beta\tanh(s)\sinh^{-1}(s)} \tag{8}$$

with ζ, μ, α, and β all to be fixed. To have the proper constants asymptotically in s requires

$$\alpha = \frac{4\pi\beta}{3\mu} \tag{9}$$

There are several constraint-based values of μ, ranging from[13,39,40] 10/81 = 0.12345679 to 0.26. For brevity we refer to ref 2 and choose the PBE value[13] μ = 0.219514973 on the basis of its performance in predicting the G3/99 test set[41] heats of formation (see below). The parameters β and ζ are determined by appealing to two exact DFT results imposed for the exact H atom density n_H. First, exact X must cancel the classical Coulomb repulsion,[42]

$$E_X[n_H] = -E_{Coul}[n_H] = -0.3125 \tag{10}$$

to remove the integer self-interaction error exactly for H and approximately otherwise. Second, the H eigenvalue must satisfy the DFT ionization potential theorem[17]

$$\varepsilon_H = -1/2 = \varepsilon_{u,HOMO}^{NCAP}[n_H] - v_X^{NCAP}(\varepsilon_{u,HOMO}^{NCAP},\zeta) \tag{11}$$

Here the "u" subscript denotes the value from the unshifted potential (for general β and ζ), which in agreement with eq 7 goes to the asymptotic constant[25]

$$\lim_{|\mathbf{r}|\to\infty} v_X^{NCAP}([n];\mathbf{r}) = \frac{{A_X}^2{Q_X}^2}{2}\left(1 + \sqrt{1 - \frac{4\varepsilon_{u,HOMO}^{NCAP}}{{A_X}^2 Q_X^2}}\right) \tag{12}$$

with A_X as defined in eq 1, $Q_X = (2^{1/2}/3(3\pi^2)^{1/3})C$, and $C = 4\pi(1-\zeta)/3$. The shift is the H atom derivative discontinuity.[17] These constraints yield β = 0.018085697 and ζ = 0.304121419.

With this value of ζ one finds, according to eq 7 with $v_X^{NCAP}(\varepsilon_{u,HOMO}^{NCAP},\ \zeta)$ instead of $v_X^{trial}(\varepsilon_{HOMO},\zeta)$, that for the hydrogen atom ground state

$$v_X^{NCAP}([n];\ r) \xrightarrow[r\to\infty]{} 0.23196 - 0.31885/r \tag{13}$$

It is expected that for any finite system in the far asymptotic region the values of these constants will be around the hydrogen atom values. Thus, the new exchange enhancement factor is denoted NCAP (nearly correct asymptotic potential) because it goes as $-c/r$ with an estimated value for the constant c of about 0.3. In Figure 1 we present the plot of

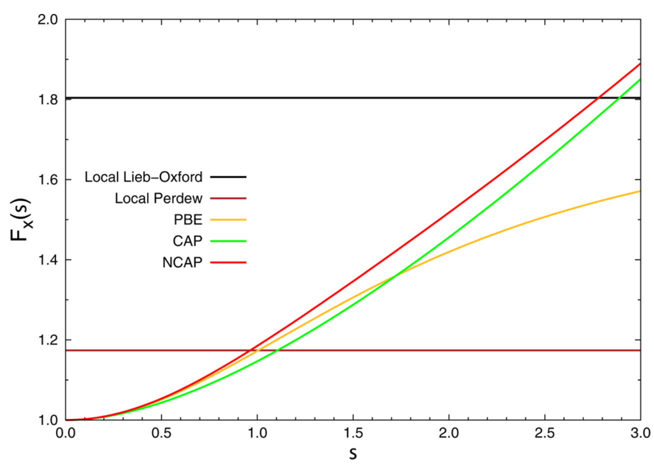

Figure 1. Comparison of $F_X^{NCAP}(s)$ enhancement factor with the original CAP version and that of PBE. Also shown are the values of the local Lieb−Oxford[63] and Perdew et al.[64] bounds.

several enhancement factors in the interval $0 \leq s \leq 3$, which corresponds to the physically important region for the total energy.[5,43−45] One can see that in this interval $F_X^{NCAP}(s)$ generally lies modestly above the original $F_X^{CAP}(s)$, while below $s \approx 1.25$, $F_X^{NCAP}(s)$ closely resembles $F_X^{PBE}(s)$.

The unshifted and shifted X potentials are $v_{X,u}^{NCAP}([n];\mathbf{r}) = \delta E_X[n]/\delta n(\mathbf{r})$ and $v_X^{NCAP}([n];\mathbf{r}) = v_{X,u}^{NCAP}([n];\mathbf{r}) - v_X^{DD}(\varepsilon_{u,HOMO}^{NCAP},\zeta)$. Figure 2 displays both of those together with the PBE X potential (the three of them calculated numerically with a modified version of the Herman−Skillman[46] code) for Ne compared to an optimized effective potential (OEP).[47,48] There is a clear improvement compared to PBE in both shape and absolute magnitudes, especially around the shell-structure kink. Note, however, that the NCAP potential tends to $-1/r$ behavior more slowly than the OEP. A proof[49] that the X potential must go asymptotically to zero substantiates the correctness of the NCAP shift. In contrast, the so-called potential adjusters (e.g., ref 50) introduce only a shift and do

DOI: 10.1021/acs.jctc.8b00998
J. Chem. Theory Comput. 2019, 15, 303−310

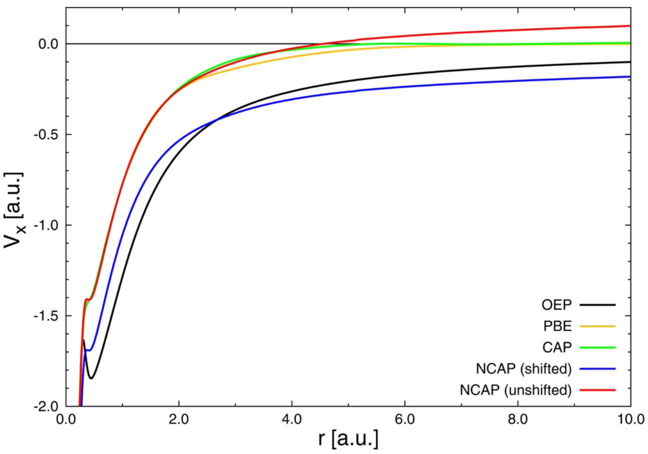

Figure 2. Exchange potential for Ne atom before and after shift of NCAP compared with the OEP, PBE, and original CAP (all unshifted).

not alter the shape of v_X. Regional splicing procedures[51−53] and Fermi−Amaldi based schemes[54,55] both shift and alter v_X but at the cost of it not being a functional derivative of a proper E_X.

An interesting comparison involves the hydrogen atom, for which Gill and Pople[56] gave a GGA with correct v_X. In Figure 3

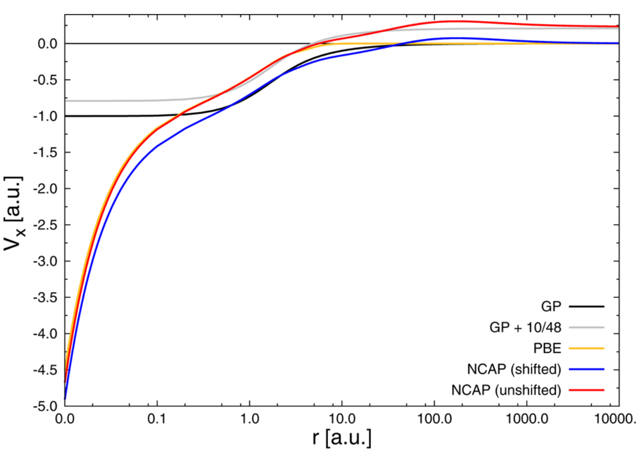

Figure 3. Comparison of the Gill and Pople exact exchange potential for the hydrogen atom with PBE and NCAP unshifted and shifted. In the plot one can also see the modification of Tozer to the Gill and Pople exchange potential (see text).

it can be seen that from about $r \sim 0.5$ au there is good agreement with the shifted NCAP v_X. In this figure one also can recognize that the new functional reduces a spurious bump in the CAP atomic exchange potential (see Figure 8b in ref 2) and moves it to distances irrelevantly far from the nucleus ($r \sim 100.0$ au). However, the X enhancement factors differ critically: $F_X^{\text{Gill−Pople}}$ is *negative* for s below about 0.1 and above about 1.8. The dominant contributions for an X GGA come in the region $0 \leq s \leq 3$.[5,43−45] For more than half that region, therefore, $F_X^{\text{Gill−Pople}}$ is qualitatively wrong. This illustrates the limitations arising when incompatible exact constraints are enforced in designing a GGA. The Gill−Pople functional works for the H atom but is completely incorrect for all other systems.

Tozer[57] considered a local hydrogenic and a Fermi−Amaldi model to obtain positive shifts of $10Z/48$ and $5Z/16$, respectively (Z is the nuclear charge), of the Gill−Pople potential for the H isoelectronic series. This was done to obtain an asymptotically nonvanishing potential. His first scheme, which gives 10/48 hartree for the atomic H shift, agrees rather well with the nonvanishing unshifted NCAP potential, as shown in Figure 3.

NCAP nearly meets a sum-rule constraint that most GGA X functionals do not,[58] namely, $\int \nabla^2 v_X([n];\mathbf{r})\, d\mathbf{r} = 4\pi$. The reason is that this sum rule is essentially electrostatic in character.[59] However, as we have discussed, the asymptotic behavior of the exchange potential is given by $v_X([n];\mathbf{r}) \xrightarrow[r\to\infty]{} -c/r$, where c has a value around 0.3, and because NCAP is singular at the nucleus, which implies that there is an additional point charge contribution,[60] in the present case, the sum rule is given by $\int \nabla^2 v_X([n];\mathbf{r})\, d\mathbf{r} = 4\pi(c + c_{\text{nuc}})$, where $c_{\text{nuc}} = -\lim_{r\to 0} r v_X([n];\mathbf{r})$. Thus, while for most GGAs this integral is equal to zero, because their exchange potential decays faster than r^{-1}, in the case of NCAP the constraint is nearly satisfied, since the integral is equal to a constant but not the exact one.

Having imposed constraints and behaviors solely related to X, what is needed for correlation is a GGA developed with regard to constraints on correlation alone. The Perdew-86 functional[61] fills that need; hence we adopt it without change. For brevity, throughout the remaining discussion "NCAP" denotes the combination of NCAP X and Perdew-86 C.

III. RESULTS AND VALIDATION

Values reported here were calculated with a modified version of NWChem 6.5[62] with the basis set choices, and databases described in refs 2 and 42, unless otherwise noted.

Because $F_X^{\text{NCAP}}(s)$ diverges as $s \to \infty$, it is possible that E_{XC}^{NCAP} energy could violate the Lieb−Oxford bound.[63] As detailed in the Supporting Information, for none of a set of 492 molecules does that happen for the global bound. In fact, even the far stricter bound of ref 64 is obeyed.

For comparison of the performance of the new XC functional with respect to others, we followed Jacob's ladder.[6] Thus, we included the LSDA[19,65] at the first level, two additional GGAs, the original CAP[2] and PBE,[13] at the second, SCAN[1] at the meta-GGA level, and B3LYP[20,66−69] and CAM-B3LYP[70] at the hyper-GGA level. The first four together with NCAP are nonempirical, while the last two are empirical.

Table 1 shows the mean average deviation (MAD) for some noble gas atoms (mean deviations, MD, are given in the Supporting Information), with respect to accurate values of the X and C energies from refs 71 and 72. The X energy values were determined through an XC calculation using the universal Gaussian basis set.[73] One sees that NCAP yields a better

Table 1. MAD for the Exchange, Correlation, and Exchange−Correlation Energies of the Noble Gas Atoms Ne, Ar, Kr, and Xe in Hartrees

	E_X	E_C	E_{XC}
LSDA	4.35	1.17	3.18
PBE	0.41	0.06	0.46
CAP	0.98	0.06	1.04
NCAP	0.20	0.14	0.07
SCAN	0.14	0.07	0.08
B3LYP	0.38	0.27	0.11
CAM-B3LYP	0.17	0.16	0.02

DOI: 10.1021/acs.jctc.8b00998
J. Chem. Theory Comput. 2019, 15, 303−310

description of the X energies by approximately a factor of 2 with respect to PBE and B3LYP and comes very close to the CAM-B3LYP, SCAN, and exact values.

Table 2 shows the MADs for several molecular properties using test sets designed specifically for each of them. For heats of formation we used the G3/99 test set[41] composed of 223 molecules. The NCAP, SCAN, and B3LYP heat of formation values are rather close; hence, NCAP provides a significantly better description than the other GGA functionals considered. For the barrier heights we used the forward and backward data for 19 hydrogen and 19 non-hydrogen transfer reactions in the HTBH38/04 and the NHTBH38/04 data sets, respectively.[74−77] The MAD results for NCAP and SCAN are very similar. Both lie about 2 kcal above the B3LYP value. For the weakly bonded systems, we used the HB6/04,[78] CT7/04,[78] DI6/04,[78] WI7/05,[76] and PPS5/05[76] data sets (31 systems), NCAP does slightly worse (about 1 kcal above) than PBE and SCAN, which are close to B3LYP and CAM-B3LYP. Bond distances from the T-82F[79] data set show that NCAP is slightly worse than PBE and SCAN, which leads to the best values for this property, even better than B3LYP and CAM-B3LYP, which are slightly better than the GGAs. Finally, Hait and Head-Gordon[80] recently have suggested that the dipole moment can be used to assess the quality of the electronic density and developed a data set with 152 molecular values for that purpose. With an aug-pc-4 basis set, in the last column of Table 2 one can see that NCAP behavior on this test is only slightly worse than SCAN, which is very close to B3LYP and CAM-B3LYP. In the Supporting Information we report the results for each molecule considered in Table 2. Also we include other properties and other tests for the density.[81]

Table 2. MAD for the Heats of Formation of the G3 Set in kcal/mol (223 Molecules), Barrier Heights of the BH76 Set of Reactions in kcal/mol, Binding Energy of Weakly Bonded Systems of the WB31 Set in kcal/mol, Bond Distances of the T-96R Set in Å, and Dipole Moments of the Hait and Head-Gordon Set in Debyes (144 Molecules)

	G3	BH	WB	BD	DM
LSDA	118.3	15.5	3.6	0.082	0.159
PBE	21.2	9.9	1.6	0.018	0.153
CAP	9.2	7.6	2.7	0.022	0.141
NCAP	6.0	8.0	2.4	0.025	0.143
SCAN	5.1	8.6	1.6	0.009	0.089
B3LYP	5.7	5.9	1.2	0.011	0.075
CAM-B3LYP	3.2	3.7	1.0	0.014	0.067

An important test of the eigenvalues is related to the ionization potential theorem,[16,17] which states that for the exact XC functional, the KS HOMO eigenvalue of a finite system is the negative of the ionization potential, $\varepsilon_{\mathrm{HOMO}} = -I$. Table 3 displays results for this test on the noble gas atoms. Hartree−Fock HOMO eigenvalues and experimental first I values[82−85] also are shown. The NCAP eigenvalues correspond to the shifted potential. On this test, the NCAP MAD is better than for any other functional, by slightly more than 30% against CAM-B3LYP and by more than a factor of 2 for all the others. A related comparison with a system-dependent XC functional with the correct asymptotic behavior developed by Gledhill and Tozer[86] is shown in the Supporting Information.

The other major aspect of interpretation and use of KS eigenvalues comes from the fact that NCAP is parametrized to treat the H atom derivative discontinuity correctly and the resulting NCAP potential shift applies to all its eigenvalues. Thus, the unphysical positive LUMO energies that plague all the other functionals are absent in shifted NCAP (See Supporting Information), although HOMO−LUMO eigenvalue differences are similar to those predicted by the other functionals.

Table 3. Comparison of the HOMO Eigenvalue with the Experimental Ionization Potential (IP) in eV for Some of the Noble Gases[a]

	Ne	Ar	Kr	Xe	MAD
LSDA	13.56	10.40	9.42	8.42	5.41
PBE	13.35	10.29	9.28	8.28	5.57
CAP	13.11	10.13	9.15	8.17	5.73
NCAP	21.19	17.44	16.19	14.92	1.76
SCAN	14.00	10.73	9.69	8.62	5.11
B3LYP	15.65	11.67	10.47	9.28	4.10
CAM-B3LYP	17.67	13.48	12.19	10.89	2.31
Hartree−Fock	23.14	16.08	14.26	12.44	0.62
exp IP	21.57	15.76	14.00	12.13	

[a]The values for NCAP correspond to the shifted exchange potential.

In addition, an advantage over all other GGAs is the concurrent applicability of NCAP, *unaltered*, to accurate molecular excitation energies and response property calculations such as static and dynamic polarizabilities and hyperpolarizabilities, determined from TDDFT.[27,28]

In Table 4 we present the MAD with respect to experimental values[87−91] that results from the calculation for valence and Rydberg excitation energies. The molecules considered were N_2 (8 v, 2 R), CO (4 v, 6 R), CH_2O (3 v, 7 R), and C_2H_4 (2 v, 8 R); the quantities in parentheses indicate the number of valence and Rydberg states calculated. One can see that NCAP leads to a better description than the other GGAs and B3LYP, and a description similar to that from CAM-B3LYP. Recent calculations of Rydberg states with SCAN[92] show trends very similar to the ones obtained with NCAP with respect to the ones obtained with other GGA functionals.

Table 4. MAD for 17 Valence and 23 Ry Excitation Energies in eV for a Test Set with Four Molecules[a]

	valence	Rydberg	total
LSDA	0.30	1.29	0.87
PBE	0.35	1.47	1.00
CAP	0.32	1.25	0.86
NCAP	0.26	0.64	0.48
B3LYP	0.40	0.88	0.68
CAM-B3LYP	0.42	0.46	0.44

[a]The values for NCAP correspond to the unshifted exchange potential.

For the static and dynamic polarizabilities we have done calculations using time-dependent auxiliary density perturbation theory[93−97] with a locally modified version of the code deMon2k 4.4.4,[98] on a test set formed by 12 molecules with a total of 62 values, 12 for the static case, and 50 for the dynamic case (see Supporting Information) for which there are accurate wave function-based calculations reported.[99,100] The MAD in au with respect to those accurate values is 4.44 for LSDA, 2.25 for PBE, 1.92 for CAP, and 1.74 for NCAP, which shows that the proposed X functional leads to the best results.

DOI: 10.1021/acs.jctc.8b00998
J. Chem. Theory Comput. 2019, 15, 303−310

It is important to note that while there is some resemblance of NCAP design objectives and choices with those relevant to the AK13 functional,[25,29−32] there are major differences in the two enhancement factors: compare eq 8 with eq 2. The consequence is that NCAP is a high-quality density functional in and of itself, as illustrated by the performance successes presented above in detail. In contrast, the AK13 functional does not deliver good energetics on its own and therefore must be used as a KS orbital generator for post-SCF LDA calculations.[30] NCAP achieves the goals of AK13 without its limitations.

IV. CONCLUDING REMARKS

To summarize, the NCAP GGA X functional requires no experimental parametrization, delivers a physically sensible X potential with approximately correct behavior at large finite distances, respects the global Lieb−Oxford bound in all cases considered thus far, delivers a potential shift that moves KS HOMO eigenvalues substantially closer to satisfaction of the ionization potential theorem than any other system-independent GGA, provides superior or competitive performance on standard thermochemical test sets, and provides performance on TD-DFT response properties equal to or better than GGAs patched for use in such calculations.

■ ASSOCIATED CONTENT

Supporting Information

The Supporting Information is available free of charge on the ACS Publications website at DOI: 10.1021/acs.jctc.8b00998.

Details of the derivation and characteristics of the exchange functional, augmented versions of the tables that appear in the article to report the MD and MAD, plot of satisfaction of the Lieb−Oxford bound by NCAP, comparison of NCAP-shifted HOMO eigenvalue with a system-dependent XC functional, comparison of the NCAP HOMO and LUMO shifted eigenvalues with those from other XC functionals, results for the individual molecules including enthalpies of formation, ionization potentials, electron and proton affinities, binding energies for weakly bonded systems, forward and backward H and non-H transfer reactions, bond lengths, vibrational frequencies, TDDFT valence and Rydberg excited states, integrated errors of density, gradient norm of the density, and Laplacian of the density, dipole moments, and polarizabilities (PDF)

■ AUTHOR INFORMATION

Corresponding Authors

*J.C.-E. E-mail: jcarmona_26@yahoo.com.mx.

*J.L.G. E-mail: jlgm@xanum.uam.mx.

ORCID

Javier Carmona-Espíndola: 0000-0001-5723-9336

José L. Gázquez: 0000-0001-6685-7080

Alberto Vela: 0000-0002-2794-8622

Notes

The authors declare no competing financial interest.

■ ACKNOWLEDGMENTS

We thank the Laboratorio Nacional de Cómputo de Alto Desempeño for the use of their facilities through the Laboratorio de Supercómputo y Visualización of Universidad Autónoma Metropolitana-Iztapalapa. J.L.G. thanks Conacyt for grant 237045, and A.V. thanks Conacyt for the Fronteras grant 867. S.B.T. was supported in part by U.S. NSF grant DMR-1515307. We thank Daniel Mejia-Rodríguez for several insightful comments.

■ REFERENCES

(1) Sun, J. W.; Ruzsinszky, A.; Perdew, J. P. Strongly Constrained and Appropriately Normed Semilocal Density Functional. *Phys. Rev. Lett.* **2015**, *115*, 036402.

(2) Carmona-Espíndola, J.; Gázquez, J. L.; Vela, A.; Trickey, S. B. Generalized gradient approximation exchange energy functional with correct asymptotic behavior of the corresponding potential. *J. Chem. Phys.* **2015**, *142*, 054105.

(3) Carmona-Espíndola, J.; Gázquez, J. L.; Vela, A.; Trickey, S. B. Temperature effects in static and dynamic polarizabilities from distinct generalized gradient approximation exchange-correlation functionals. *Chem. Phys. Lett.* **2016**, *664*, 77−82.

(4) Pacheco-Kato, J. C.; del Campo, J. M.; Gázquez, J. L.; Trickey, S. B.; Vela, A. A PW91-like exchange with a simple analytical form. *Chem. Phys. Lett.* **2016**, *651*, 268−273.

(5) Gázquez, J. L.; del Campo, J. M.; Trickey, S. B.; Alvarez-Mendez, R. J.; Vela, A., Analysis of Generalized Gradient Approximation for Exchange Energy. In *Concepts and Methods in Modern Theoretical Chemistry*; Ghosh, S. K., Chattaraj, P. K., Eds.; CRC Press: Boca Raton FL, 2013; pp 295−311.

(6) Perdew, J. P.; Schmidt, K. In *Density Functional Theory and its Application to Materials*; Van Doren, V. E., Van Alsenoy, C., Geerlings, P., Eds.; AIP: Melville: New York, 2001; pp 1−20.

(7) Karasiev, V. V.; Chakraborty, D.; Trickey, S. B. In *Many-electron Approaches in Physics, Chemistry, and Mathematics: A Multidisciplinary View*; Delle Site, L., Bach, V., Eds.; Springer: Heidelberg, 2014; pp 113−134.

(8) Perdew, J. P.; Kurth, S. Density Functionals for Non-relativistic Coulomb Systems in the New Century. In *A Primer in Density Functional Theory*; Fiolhais, C., Nogueira, F., Marques, M. A. L., Eds.; Springer: Berlin, 2003; pp 1−55.

(9) Scuseria, G. E.; Staroverov, V. N. Progress in the development of exchange-correlation functionals. In *Theory and Applications of Computational Chemistry: The First Forty Years*; Dykstra, C., Frenking, G., Kim, K. S., Scuseria, G. E., Eds.; Elsevier: Amsterdam, 2005; pp 669−724.

(10) Burke, K. Perspective on density functional theory. *J. Chem. Phys.* **2012**, *136*, 150901.

(11) Cohen, A. J.; Mori-Sanchez, P.; Yang, W. T. Challenges for Density Functional Theory. *Chem. Rev.* **2012**, *112*, 289−320.

(12) Becke, A. D. Perspective: Fifty years of density-functional theory in chemical physics. *J. Chem. Phys.* **2014**, *140*, 18A301.

(13) Perdew, J. P.; Burke, K.; Ernzerhof, M. Generalized gradient approximation made simple. *Phys. Rev. Lett.* **1996**, *77*, 3865−3868;Erratum *Phys. Rev. Lett.* **1997**, *78*, 1396.

(14) Perdew, J. P.; Levy, M. Physical Content of the Exact Kohn-Sham Orbital Energies - Band-Gaps and Derivative Discontinuities. *Phys. Rev. Lett.* **1983**, *51*, 1884−1887.

(15) Sham, L. J.; Schluter, M. Density-Functional Theory of the Energy-Gap. *Phys. Rev. Lett.* **1983**, *51*, 1888−1891.

(16) Levy, M.; Perdew, J. P.; Sahni, V. Exact Differential-Equation for the Density and Ionization-Energy of A Many-Particle System. *Phys. Rev. A: At., Mol., Opt. Phys.* **1984**, *30*, 2745−2748.

(17) Perdew, J. P.; Levy, M. Comment on "Significance of the highest occupied Kohn-Sham eigenvalue". *Phys. Rev. B: Condens. Matter Mater. Phys.* **1997**, *56*, 16021−16028.

(18) Perdew, J. P.; Yue, W. Accurate and Simple Density Functional for the Electronic Exchange Energy - Generalized Gradient Approximation. *Phys. Rev. B: Condens. Matter Mater. Phys.* **1986**, *33*, 8800−8802.

(19) Dirac, P. A. M. Note on exchange phenomena in the Thomas atom. *Math. Proc. Cambridge Philos. Soc.* **1930**, *26*, 376−385.

(20) Becke, A. D. Density-Functional Exchange-Energy Approximation with Correct Asymptotic-Behavior. *Phys. Rev. A: At., Mol., Opt. Phys.* **1988**, *38*, 3098−3100.
(21) Engel, E.; Chevary, J. A.; Macdonald, L. D.; Vosko, S. H. Asymptotic Properties of the Exchange Energy Density and the Exchange Potential of Finite Systems: Relevance for Generalized Gradient Approximations. *Z. Phys. D: At., Mol. Clusters* **1992**, *23*, 7−14.
(22) Levy, M.; Perdew, J. P. Tight Bound and Convexity Constraint on the Exchange-Correlation-Energy Functional in the Low-Density Limit, and Other Formal Tests of Generalized-Gradient Approximations. *Phys. Rev. B: Condens. Matter Mater. Phys.* **1993**, *48*, 11638−11645.
(23) Vela, A.; Medel, V.; Trickey, S. B. Variable Lieb-Oxford bound satisfaction in a generalized gradient exchange-correlation functional. *J. Chem. Phys.* **2009**, *130*, 244103.
(24) Vela, A.; Pacheco-Kato, J. C.; Gázquez, J. L.; Mdel Campo, J. M.; Trickey, S. B. Improved constraint satisfaction in a simple generalized gradient approximation exchange functional. *J. Chem. Phys.* **2012**, *136*, 144115.
(25) Armiento, R.; Kummel, S. Orbital Localization, Charge Transfer, and Band Gaps in Semilocal Density-Functional Theory. *Phys. Rev. Lett.* **2013**, *111*, 036402.
(26) Li, S. H. L.; Truhlar, D. G. Improving Rydberg Excitations within Time-Dependent Density Functional Theory with Generalized Gradient Approximations: The Exchange-Enhancement-for-Large-Gradient Scheme. *J. Chem. Theory Comput.* **2015**, *11*, 3123−3130.
(27) Petersilka, M.; Gossmann, U. J.; Gross, E. K. U. Excitation energies from time-dependent density-functional theory. *Phys. Rev. Lett.* **1996**, *76*, 1212−1215.
(28) Casida, M. E., Time-Dependent Density Functional Response Theory of Molecular Systems: Theory, Computational Methods, and Functionals. In *Recent Developments and Applications of Modern Density Functional Theory*; Seminario, J. M., Ed.; Elsevier Science B. V.: Amsterdam, 1996; pp 391−439.
(29) Vlcek, V.; Steinle-Neumann, G.; Leppert, L.; Armiento, R.; Kummel, S. Improved ground-state electronic structure and optical dielectric constants with a semilocal exchange functional. *Phys. Rev. B: Condens. Matter Mater. Phys.* **2015**, *91*, 035107.
(30) Lindmaa, A.; Armiento, R. Energetics of the AK13 semilocal Kohn-Sham exchange energy functional. *Phys. Rev. B: Condens. Matter Mater. Phys.* **2016**, *94*, 155143.
(31) Aschebrock, T.; Armiento, R.; Kummel, S. Orbital nodal surfaces: Topological challenges for density functionals. *Phys. Rev. B: Condens. Matter Mater. Phys.* **2017**, *95*, 245118.
(32) Aschebrock, T.; Armiento, R.; Kummel, S. Challenges for semilocal density functionals with asymptotically nonvanishing potentials. *Phys. Rev. B: Condens. Matter Mater. Phys.* **2017**, *96*, 075140.
(33) Antaya, H.; Zhou, Y. X.; Ernzerhof, M. Approximating the exchange energy through the nonempirical exchange-factor approach. *Phys. Rev. A: At., Mol., Opt. Phys.* **2014**, *90*, 032513.
(34) Perdew, J. P.; Chevary, J. A.; Vosko, S. H.; Jackson, K. A.; Pederson, M. R.; Singh, D. J.; Fiolhais, C. Atoms, Molecules, Solids, and Surfaces - Applications of the Generalized Gradient Approximation for Exchange and Correlation. *Phys. Rev. B: Condens. Matter Mater. Phys.* **1992**, *46*, 6671−6687;Erratum *Phys. Rev. B: Condens. Matter Mater. Phys.* **1993**, *48*, 4978.
(35) Hoffmann-Ostenhof, M.; Hoffmann-Ostenhof, T. Schrodinger inequalities and asymptotic behavior of electron density of atoms and molecules. *Phys. Rev. A: At., Mol., Opt. Phys.* **1977**, *16*, 1782−1785.
(36) Tal, Y. Asymptotic behavior of ground state charge density in atoms. *Phys. Rev. A: At., Mol., Opt. Phys.* **1978**, *18*, 1781−1783.
(37) Yang, W. T.; Cohen, A. J.; Mori-Sanchez, P. Derivative discontinuity, bandgap and lowest unoccupied molecular orbital in density functional theory. *J. Chem. Phys.* **2012**, *136*, 204111.
(38) Mosquera, M. A.; Wasserman, A. Derivative discontinuities in density functional theory. *Mol. Phys.* **2014**, *112*, 2997−3013.
(39) Antoniewicz, P. R.; Kleinman, L. Kohn-Sham Exchange Potential Exact to 1 St Order in Rho(K)/Rho0. *Phys. Rev. B: Condens. Matter Mater. Phys.* **1985**, *31*, 6779−6781.
(40) Constantin, L. A.; Fabiano, E.; Laricchia, S.; Della Sala, F. Semiclassical Neutral Atom as a Reference System in Density Functional Theory. *Phys. Rev. Lett.* **2011**, *106*, 186406.
(41) Curtiss, L. A.; Raghavachari, K.; Redfern, P. C.; Pople, J. A. Assessment of Gaussian-3 and density functional theories for a larger experimental test set. *J. Chem. Phys.* **2000**, *112*, 7374−7383.
(42) del Campo, J. M.; Gázquez, J. L.; Trickey, S. B.; Vela, A. Non-empirical improvement of PBE and its hybrid PBE0 for general description of molecular properties. *J. Chem. Phys.* **2012**, *136*, 104108.
(43) Zupan, A.; Burke, K.; Ernzerhof, M.; Perdew, J. P. Distributions and averages of electron density parameters: Explaining the effects of gradient corrections. *J. Chem. Phys.* **1997**, *106*, 10184−10193.
(44) Zupan, A.; Perdew, J. P.; Burke, K.; Causà, M. Density-gradient analysis for density functional theory: Application to atoms. *Int. J. Quantum Chem.* **1997**, *61*, 835−845.
(45) del Campo, J. M.; Gázquez, J. L.; Alvarez-Mendez, R. J.; Vela, A. The Reduced Density Gradient in Atoms. *Int. J. Quantum Chem.* **2012**, *112*, 3594−3598.
(46) Herman, F.; Skillman, S. *Atomic Structure Calculations*; Prentice-Hall: Englewood Cliffs, NJ, 1963.
(47) Talman, J. D.; Shadwick, W. F. Optimized Effective Atomic Central Potential. *Phys. Rev. A: At., Mol., Opt. Phys.* **1976**, *14*, 36−40.
(48) Engel, E.; Vosko, S. H. Accurate optimized potential model solutions for spherical spin-polarized atoms: Evidence for limitations of the exchange-only local spin density and generalized gradient approximations. *Phys. Rev. A: At., Mol., Opt. Phys.* **1993**, *47*, 2800−2811.
(49) Pino, R. Analysis of exchange and exchange-correlation potentials with non-zero constant asymptotics. *J. Mol. Struct.: THEOCHEM* **2003**, *624*, 13−16.
(50) Gorling, A. Exchange-correlation potentials with proper discontinuities for physically meaningful Kohn-Sham eigenvalues and band structures. *Phys. Rev. B: Condens. Matter Mater. Phys.* **2015**, *91*, 245120.
(51) Tozer, D. J.; Handy, N. C. Improving virtual Kohn-Sham orbitals and eigenvalues: Application to excitation energies and static polarizabilities. *J. Chem. Phys.* **1998**, *109*, 10180−10189.
(52) Casida, M. E.; Salahub, D. R. Asymptotic correction approach to improving approximate exchange-correlation potentials: Time-dependent density-functional theory calculations of molecular excitation spectra. *J. Chem. Phys.* **2000**, *113*, 8918−8935.
(53) Gázquez, J. L.; Garza, J.; Vargas, R.; Vela, A. An exchange-correlation potential with built in discontinuity and correct long range behavior. In *CP979 Recent Developments in Physical Chem. 3rd Mexican Meeting on Mathematical and Experimental Physics*; Diaz-Herrera, E., Juaristi, E., Eds.; AIP: New York, 2008; Vol. 979, pp 11−20.
(54) Ayers, P. W.; Morrison, R. C.; Parr, R. G. Fermi-Amaldi model for exchange-correlation: atomic excitation energies from orbital energy differences. *Mol. Phys.* **2005**, *103*, 2061−2072.
(55) Pan, C. R.; Fang, P. T.; Chai, J. D. Asymptotic correction schemes for semilocal exchange-correlation functionals. *Phys. Rev. A: At., Mol., Opt. Phys.* **2013**, *87*, 052510.
(56) Gill, P. M. W.; Pople, J. A. Exact exchange functional for the hydrogen atom. *Phys. Rev. A: At., Mol., Opt. Phys.* **1993**, *47*, 2383−2385.
(57) Tozer, D. J. Exact hydrogenic density functionals. *Phys. Rev. A: At., Mol., Opt. Phys.* **1997**, *56*, 2726−2730.
(58) Ayers, P. W.; Levy, M. Sum rules for exchange and correlation potentials. *J. Chem. Phys.* **2001**, *115*, 4438−4443.
(59) Liu, S. B.; Ayers, P. W.; Parr, R. G. Alternative definition of exchange-correlation charge in density functional theory. *J. Chem. Phys.* **1999**, *111*, 6197−6203.
(60) Kohut, S. V.; Staroverov, V. N. Apparent violation of the sum rule for exchange-correlation charges by generalized gradient approximations. *J. Chem. Phys.* **2013**, *139*, 164117.

(61) Perdew, J. P. Density-Functional Approximation for the Correlation-Energy of the Inhomogeneous Electron-Gas. *Phys. Rev. B: Condens. Matter Mater. Phys.* **1986**, *33*, 8822−8824.
(62) Valiev, M.; Bylaska, E. J.; Govind, N.; Kowalski, K.; Straatsma, T. P.; Van Dam, H. J. J.; Wang, D.; Nieplocha, J.; Apra, E.; Windus, T. L.; de Jong, W. NWChem: A comprehensive and scalable open-source solution for large scale molecular simulations. *Comput. Phys. Commun.* **2010**, *181*, 1477−1489.
(63) Lieb, E. H.; Oxford, S. Improved Lower Bound on the Indirect Coulomb Energy. *Int. J. Quantum Chem.* **1981**, *19*, 427−439.
(64) Perdew, J. P.; Ruzsinszky, A.; Sun, J. W.; Burke, K. Gedanken densities and exact constraints in density functional theory. *J. Chem. Phys.* **2014**, *140*, 18A533.
(65) Vosko, S. H.; Wilk, L.; Nusair, M. Accurate Spin-Dependent Electron Liquid Correlation Energies for Local Spin-Density Calculations - A Critical Analysis. *Can. J. Phys.* **1980**, *58*, 1200−1211.
(66) Becke, A. D. *J. Chem. Phys.* **1993**, *98*, 5648−5652.
(67) Lee, C. T.; Yang, W. T.; Parr, R. G. Development of the Colle-Salvetti Correlation-Energy Formula Into A Functional of the Electron-Density. *Phys. Rev. B: Condens. Matter Mater. Phys.* **1988**, *37*, 785−789.
(68) Kim, K.; Jordan, K. D. *J. Phys. Chem.* **1994**, *98*, 10089−10094.
(69) Stephens, P. J.; Devlin, F. J.; Chabalowski, C. F.; Frisch, M. J. *J. Phys. Chem.* **1994**, *98*, 11623−11627.
(70) Yanai, T.; Tew, D. P.; Handy, N. C. A new hybrid exchange-correlation functional using the Coulomb-attenuating method (CAM-B3LYP). *Chem. Phys. Lett.* **2004**, *393*, 51−57.
(71) Chakravorty, S. J.; Gwaltney, S. R.; Davidson, E. R.; Parpia, F. A.; Fischer, C. F. Ground state correlation energies for atomic ions with 3 to 18 electrons. *Phys. Rev. A: At., Mol., Opt. Phys.* **1993**, *47*, 3649−3670.
(72) McCarthy, S. P.; Thakkar, A. J. Accurate all-electron correlation energies for the closed-shell atoms from Ar to Rn and their relationship to the corresponding MP2 correlation energies. *J. Chem. Phys.* **2011**, *134*, 044102.
(73) de Castro, E. V. R.; Jorge, F. E. Accurate universal gaussian basis set for all atoms of the periodic table. *J. Chem. Phys.* **1998**, *108*, 5225−5229.
(74) Zhao, Y.; Gonzalez-Garcia, N.; Truhlar, D. G. Benchmark database of barrier heights for heavy atom transfer, nucleophilic substitution, association, and unimolecular reactions and its use to test theoretical methods. *J. Phys. Chem. A* **2005**, *109*, 2012−2018.
(75) Zhao, Y.; Lynch, B. J.; Truhlar, D. G. Multi-coefficient extrapolated density functional theory for thermochemistry and thermochemical kinetics. *Phys. Chem. Chem. Phys.* **2005**, *7*, 43−52.
(76) Zhao, Y.; Truhlar, D. G. Design of density functionals that are broadly accurate for thermochemistry, thermochemical kinetics, and nonbonded interactions. *J. Phys. Chem. A* **2005**, *109*, 5656−5667.
(77) Peverati, R.; Truhlar, D. G. The quest for a universal density functional: The accuracy of density functionals across a broad spectrum of databases in chemistry and physics. *arXiv:1212.0944v4 [physics.chem-ph]*, 2013.
(78) Zhao, Y.; Truhlar, D. G. Benchmark databases for nonbonded interactions and their use to test density functional theory. *J. Chem. Theory Comput.* **2005**, *1*, 415−432.
(79) Staroverov, V. N.; Scuseria, G. E.; Tao, J. M.; Perdew, J. P. Comparative assessment of a new nonempirical density functional: Molecules and hydrogen-bonded complexes. *J. Chem. Phys.* **2003**, *119*, 12129−12137.
(80) Hait, D.; Head-Gordon, M. How Accurate Is Density Functional Theory at Predicting Dipole Moments? An Assessment Using a New Database of 200 Benchmark Values. *J. Chem. Theory Comput.* **2018**, *14*, 1969−1981.
(81) Medvedev, M. G.; Bushmarinov, I. S.; Sun, J. W.; Perdew, J. P.; Lyssenko, K. A. Density functional theory is straying from the path toward the exact functional. *Science* **2017**, *355*, 49−52.
(82) Saloman, E. B.; Sansonetti, C. J. Wavelengths, energy level classifications, and energy levels for the spectrum of neutral neon. *J. Phys. Chem. Ref. Data* **2004**, *33*, 1113−1158.
(83) Velchev, I.; Hogervorst, W.; Ubachs, W. Precision VUV spectroscopy of ArI at 105 nm. *J. Phys. B: At., Mol. Opt. Phys.* **1999**, *32*, L511−L516.
(84) Saloman, E. B. Energy levels and observed spectral lines of krypton, KrI through Kr XXXVI. *J. Phys. Chem. Ref. Data* **2007**, *36*, 215−386.
(85) Saloman, E. B. Energy levels and observed spectral lines of xenon, Xe I through Xe LIV. *J. Phys. Chem. Ref. Data* **2004**, *33*, 765−921.
(86) Gledhill, J. D.; Tozer, D. J. System-dependent exchange-correlation functional with exact asymptotic potential and epsilon-(HOMO) approximate to -I. *J. Chem. Phys.* **2015**, *143*, 024104.
(87) Ben-Shlomo, S. B.; Kaldor, U. N-2 excitations below 15 eV by multireference coupled-cluster method. *J. Chem. Phys.* **1990**, *92*, 3680−3682.
(88) Huber, K. P.; Herzberg, G. *Molecular Spectra and Molecular Structure IV. Constants of Diatomic Molecules*; Van Nostrand: New York, 1979.
(89) Nielsen, E. S.; Jorgensen, P.; Oddershede, J. Transition moments and dynamic polarizabilities in a 2nd order polarization propagator approach. *J. Chem. Phys.* **1980**, *73*, 6238−6246.
(90) Clouthier, D. J.; Ramsay, D. A. The spectroscopy of formaldehyde and thioformaldehyde. *Annu. Rev. Phys. Chem.* **1983**, *34*, 31−58.
(91) Serrano-Andrés, L.; Merchan, M.; Nebotgil, I.; Lindh, R.; Roos, B. O. Towards an accurate molecular orbital theory for excited states - ethene,butadiene, and hexatriene. *J. Chem. Phys.* **1993**, *98*, 3151−3162.
(92) Tozer, D. J.; Peach, M. J. G. Molecular excited states from the SCAN functional. *Mol. Phys.* **2018**, *116*, 1504−1511.
(93) Shedge, S. V.; Carmona-Espíndola, J.; Pal, S.; Köster, A. M. Comparison of the Auxiliary Density Perturbation Theory and the Noniterative Approximation to the Coupled Perturbed Kohn-Sham Method: Case Study of the Polarizabilities of Disubstituted Azoarene Molecules. *J. Phys. Chem. A* **2010**, *114*, 2357−2364.
(94) Carmona-Espíndola, J.; Flores-Moreno, R.; Köster, A. M. Time-dependent auxiliary density perturbation theory. *J. Chem. Phys.* **2010**, *133*, 084102.
(95) Carmona-Espíndola, J.; Flores-Moreno, R.; Köster, A. M. Static and dynamic first hyperpolarizabilities from time-dependent auxiliary density perturbation theory. *Int. J. Quantum Chem.* **2012**, *112*, 3461−3471.
(96) Calaminici, P.; Carmona-Espíndola, J.; Geudtner, G.; Köster, A. M. Static and dynamic polarizability of C-540 fullerene. *Int. J. Quantum Chem.* **2012**, *112*, 3252−3255.
(97) Shedge, S. V.; Pal, S.; Köster, A. M. Theoretical study of frequency and temperature dependence of dipole-quadrupole polarizability of P-4 and adamantane. *Chem. Phys. Lett.* **2012**, *552*, 146−150.
(98) Geudtner, G.; Calaminici, P.; Carmona-Espíndola, J.; del Campo, J. M.; Dominguez-Soria, V. D.; Flores-Moreno, R.; Gamboa, G. U.; Goursot, A.; Köster, A. M.; Reveles, J. U.; Mineva, T.; Vasquez-Perez, J. M.; Vela, A.; Zuñiga-Gutierrez, B.; Salahub, D. R. *Wiley Interdiscip. Rev.: Comput. Mol. Sci.* **2012**, *2*, 548−555.
(99) Reinsch, E. A. Calculation of dynamic polarizabilities of He, H2, Ne, HF, H2O, NH3 and CH4 with MC-SCF wavefunctions. *J. Chem. Phys.* **1985**, *83*, 5784−5791.
(100) Rozyczko, P. B.; Perera, S. A.; Nooijen, M.; Bartlett, R. J. Correlated calculations of molecular dynamic polarizabilities. *J. Chem. Phys.* **1997**, *107*, 6736−6747.

■ NOTE ADDED AFTER ASAP PUBLICATION

This paper published ASAP on December 13, 2018 with a production error in eq 13. The corrected article was reposted on December 14, 2018.

DOI: 10.1021/acs.jctc.8b00998
J. Chem. Theory Comput. 2019, 15, 303−310